LARGE SCALE STRUCTURE AFTER COBE: PECULIAR VELOCITIES AND CORRELATIONS OF COLD DARK MATTER HALOS[1]

WOJCIECH H. ZUREK
Theoretical Astrophysics, Los Alamos National Laboratory, Los Alamos, NM 87545
PETER J. QUINN
Mount Stromlo Observatory, PB Weston Creek, ACT 2611, Australia
JOHN K. SALMON
Caltech Concurrent Supercomputing Facility, 206-49, Pasadena, CA 91125
MICHAEL S. WARREN[2]
Theoretical Astrophysics, Los Alamos National Laboratory, Los Alamos, NM 87545

ABSTRACT

Large N-body simulations on parallel supercomputers allow one to simultaneously investigate large scale structure and the formation of galactic halos with unprecedented resolution. Our study shows that the masses as well as spatial distribution of halos on scales of tens of megaparsecs in a cold dark matter (CDM) Universe with the spectrum normalized to the anisotropies detected by COBE is compatible with the observations. We also show that the average value of the relative pairwise velocity dispersion σ_v — used as a principal argument against COBE-normalized CDM models — is significantly lower for halos than for individual particles. When the observational methods of extracting σ_v are applied to the redshift catalogs obtained from the numerical experiments, estimates differ significantly between different observation-sized samples, and overlap observational estimates obtained following the same procedure.

1. INTRODUCTION

Numerical studies of the cold dark matter scenario were first conducted nearly a decade ago (Davis et al., 1985). These early studies typically used $\sim 10^4$ particles and had limited dynamical range, which made it impossible to simultaneously model structure formation on both the large and small (galactic) scales. The situation has improved in the course of the intervening decade (Couchman & Carlberg, 1992; Bertschinger & Gelb, 1991; Suginohara et al., 1991; Villumsen, 1989). However, even these relatively recent simulations often lack resolution on either small or large scales. Consequently, in the numerical simulations of large scale structure one has often been reduced to guessing which of the particles should be regarded as halos, while in the high resolution simulations one had to assess the effect of the (missing) large scale power. Recent studies of CDM with gas — which shed important new light on some aspects of galaxy formation — continue to suffer from the lack of resolution on either sub-Mpc scales (Cen & Ostriker, 1992) or scales ≥ 10 Mpc (Katz et al., 1992).

Motivated in part by the Cosmic Microwave Background Explorer (COBE) detection of anisotropies in the cosmic microwave background which removes much of the ambiguity in the normalization of the CDM power spectrum, we have carried out large dissipationless N-body simulations of structure formation in spherical fragments of the de Sitter Universe, 100 and 250 Mpc in diameter. The initial density perturbations were characterized by the cold dark matter spectrum with a baryon fraction of

---

[1]LA-UR 93-2104

[2]Department of Physics, University of California, Santa Barbara

$\Omega_B = 0.05$ (Holtzman, 1989) normalized to several values of $\langle(\delta M/M)^2\rangle^{1/2}_{8\ h^{-1}\mathrm{Mpc}} = \sigma_8$ scattered around the COBE quadrupole amplitude $Q = 15.3\mu K$ (Smoot et al., 1992; Efstathiou et al., 1992). Throughout we adopt the formalism of Efstathiou et al. (1992) where the COBE Q corresponds to $\sigma_8 = 1.06$ in linear theory.

We have used a treecode algorithm somewhat similar to that originally introduced by Barnes & Hut (1986) which runs on highly parallel supercomputers. All of the runs reported here were carried out on the 512 processor Intel Touchstone Delta system at Caltech. A more detailed discussion of our code and of its performance can be found elsewhere (Warren & Salmon, 1993; Warren & Salmon, 1992). A combination of treecode software and a massively parallel computer allow us to use enough particles (N $\sim$ 17.2×10^6 or 8.8×10^6) to be able to directly identify halos as collapsed objects at $z = 0$, in a computational volume large enough to accurately model the CDM spectrum. In addition, we use a relatively small softening parameter of 20 kpc, which gives us roughly four orders of magnitude in dynamical range. This is sufficient to accurately model the collapse, dynamics and mergers of the dark matter halos which have formed in abundance in our simulations. More than 10^4 halos (with central density no less than 10^4 above background, and typically tens to hundreds of particles each) form per run by the "present" $z = 0$.

We begin our discussion with a brief review of the computational methods, and of the model. Results of our simulations are summarized in section 3. The core of that section (and of this paper) is the discussion of our results concerning small-scale peculiar velocities of CDM halos. This is the subject of section 3.2 where pairwise (radial) peculiar velocity dispersions are computed both with a full three-dimensional knowledge of halo positions and velocities, as well as from the limited information available to observers — angular positions and redshifts only. Furthermore, having calibrated our method of determining σ_v from the numerical data in numerical simulations, we then re-analyze the CfA Northern Sky Survey, and conclude (contrary to the widespread belief) that σ_v derived from that sample (or from other samples of similar size) cannot be straightforwardly used to put meaningful constraints on the small-scale power content of the models. In particular, both the slightly undernormalized CDM model and the CfA Northern Sky survey yield $\sigma_v \propto 600$ km/s. To obtain σ_v close to the usually quoted, lower $\sigma_v = 340 \pm 40$ km/s from that catalog, a special treatment of the Virgo cluster (either subtraction of Virgocentric infall or elimination of the Virgo core) seems necessary. We conclude section 3 by noting that σ_v (at least for samples of that size) is not a very reliable statistic, as σ_v appears to have a larger confidence interval than expected. Moreover, simple assumptions concerning the distribution of peculiar velocities essential in the analysis are reviewed and found lacking, especially on 5–10 Mpc (and presumably larger) scales, where the distribution of peculiar velocities is noticeably skewed.

Our conclusions concerning peculiar velocities and CDM are summarized in the last two sections of the paper, where we observe (to our surprise, and somewhat contrary to popular belief) that cold dark matter appears to be a viable model of structure formation, especially when the somewhat smaller value of $\sigma_8 = 0.7$ is adopted (which is not only consistent with the COBE measurement, but is actually favored when the inflationary origins of the CDM spectrum are properly taken into account).

2. INITIAL CONDITIONS AND COMPUTATIONAL METHODS

Table 1 summarizes the parameters of the CDM models presented in this paper. Models cdm250a and cdm100 were evolved using the same code as the one employed in Warren et al. (1992). The other two models (which are actually two stages of evolution in the same simulation) used a new, more accurate implementation of the oct-tree algorithm which analytically guarantees a user specified accuracy bound for each multipole interaction (Salmon & Warren, 1994). Particles were distributed

Label	N	R_0 (Mpc)	Q (μK)	z_i	σ_8^{linear}	σ_8^{mass}	σ_8^{halos}	σ_v^{halos}
cdm250a	17158608	125	9.5	55.5	0.67	0.78	0.68	610
cdm250b	8783482	125	23.2	110.2	1.61	1.65	1.04	1550
cdm250c	8783482	125	14.6	68.8	1.01	1.06	0.76	790
cdm100	17154598	50	10.9	62.3	0.75	0.64	0.52	690

Table 1: Model parameters for the four CDM runs presented. The values for Q follow the definition of Efstathiou, Bond and White (1992). Values for σ_8^{linear} are for the Efstathiou, Bond and White CDM spectrum integrated over an infinite k space. Actual model initial amplitudes are within 5% of these values at 8 $h^{-1}Mpc$. Values for σ_v in km/s measured at 1 h^{-1} Mpc, which have been corrected for the mean infall.

initially in a sphere. Density perturbations were introduced by varying the masses of particles. The initial redshift was chosen so that the rms deviation of the particle mass was roughly 0.2. This value keeps the particle mass dispersion small enough that two-body relaxation effects are not significantly increased above that which would occur for equal mass particles. Initial conditions introduced in this manner (without peculiar velocities) contain both growing and decaying modes, and this was taken into account so that the data shown in Table 1 refer to the growing mode only. The early-time (linear) growth of the mass fluctuations was consistent with that expected from linear theory modulo small differences in the shapes of the CDM spectra used by Efstathiou et al. (1992) and Holtzman (1989). The early time evolution of the systems used an integrator with a time variable $p \propto \log(t)$ (so the timesteps grow in proportion to t) and a smoothing length of 200 kpc (in comoving coordinates). At $z = 10$ the time variable was returned to the physical time coordinate with a uniform time step of 20 million years, and smoothing was fixed in physical coordinates at 20 kpc. The constant of proportionality in the early time integration variable is adjusted so that the timestep at $z = 10$ is matched to the desired late-time physical timestep. This allows the timestep and smoothing length to go from the early time scheme to the physical scheme in a continuous manner. The simulations used 650–750 timesteps each. Average particle masses varied from $2.11 \times 10^9 M_\odot$ for the high-resolution cdm100 model to $3.31 \times 10^{10} M_\odot$ and $6.47 \times 10^{10} M_\odot$ for the cdm250 models. This allows us an unprecedented combination of small scale resolution without truncation of large scale power. All models were run with $\Omega = 1$ and $H_0 = 50 km\ s^{-1} Mpc^{-1}$, and all distances quoted assume this value for H_0.

Halos were identified by assigning a density averaged over a 20 kpc scale (with an L_4 spline kernel) to every particle, and then selecting a spatially disjoint set of halos by considering the list of particles in order from largest density to some arbitrary cutoff density, which was about 10^4 times the background density. The method effectively progresses outward along the isodensity contours of the halos, defining the center of mass and center of mass velocity of the group of particles as the halo position and velocity. Only halos with at least 10 particles within the cutoff density were considered for further analysis. Halo masses can be then computed using the cores defined in the manner described above, by adding the masses of all particles either within a fixed radius or within a sphere of a fixed overdensity. Masses below are defined by fixing the radius of the sphere at 100 kpc. The outer 30% of the volume (near the edge of the spherical distribution) was excluded from the sample. This corresponds to a buffer region of about 15 Mpc for the 125 Mpc radius runs, and about 5 Mpc for the 50 Mpc radius run.

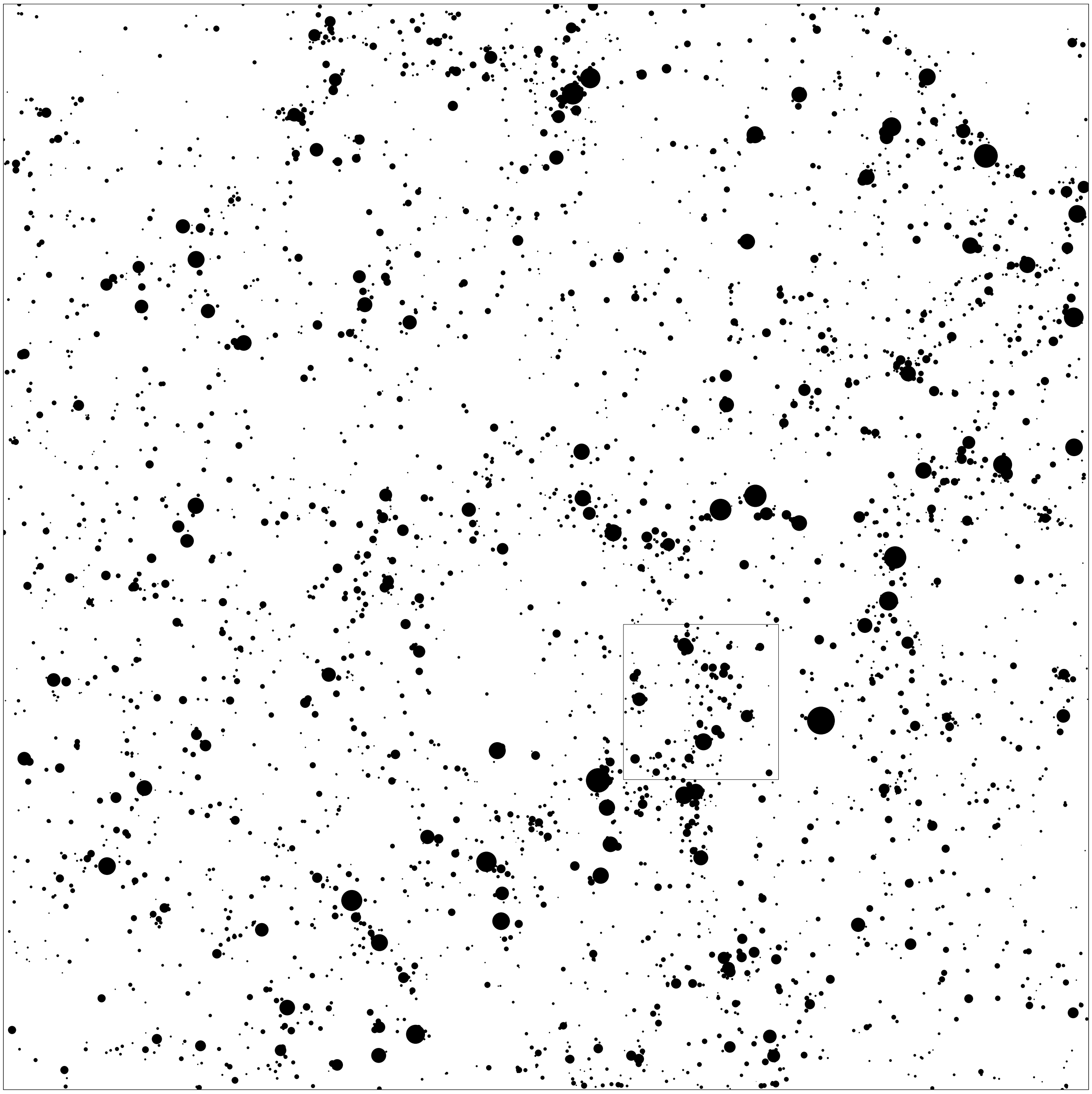

Figure 1: A plot of the projected locations of "galactic halos" in model cdm250c. The size of the square is about 180 Mpc across. Sizes of the dots are approximately proportional to the masses of the halos. The small square indicates the region which is shown in more detail in Fig. 2.

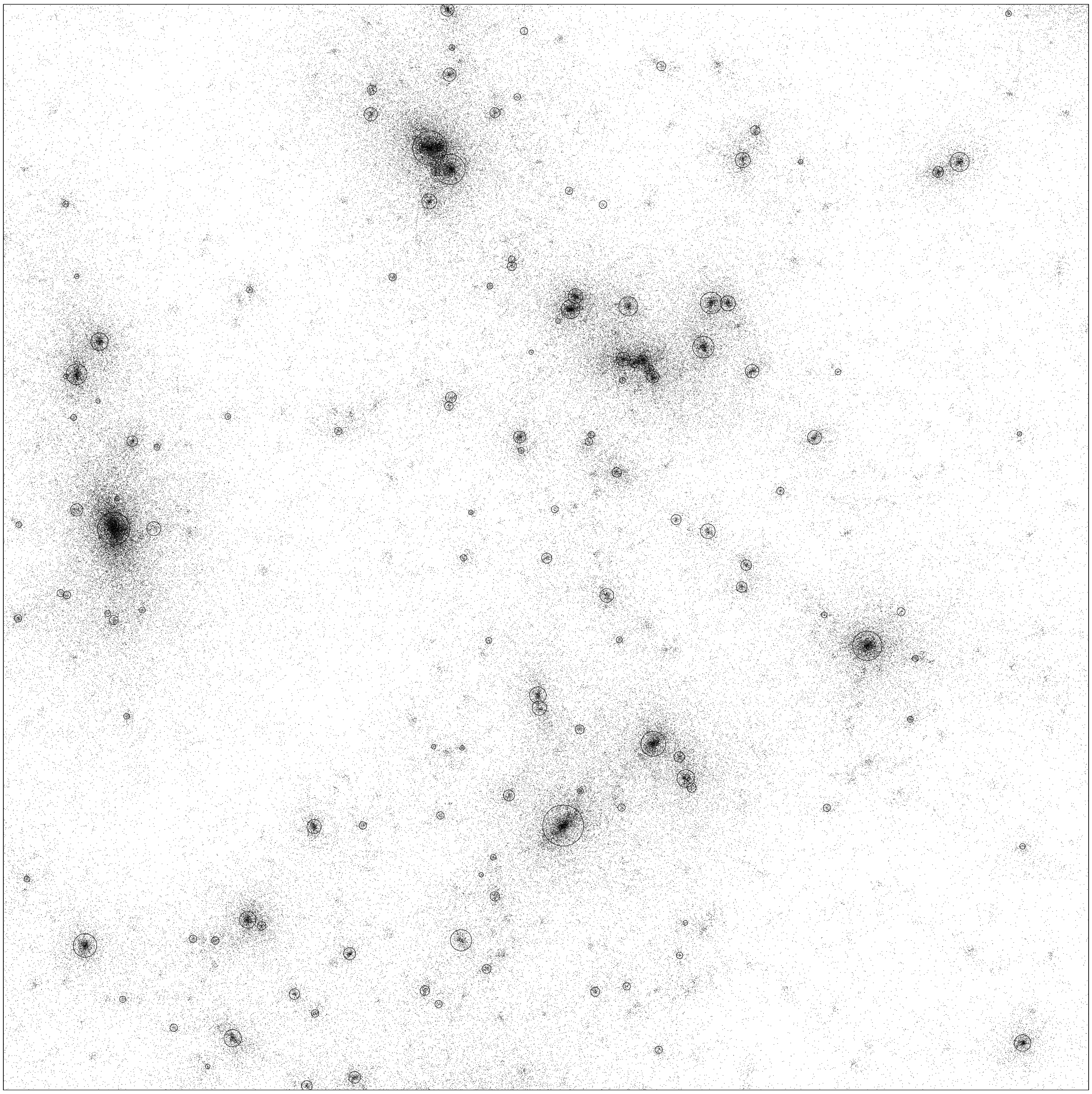

Figure 2: A high-resolution plot of every particle (about 250,000 of them) in one 50th of the total system (indicated by the small square in Fig. 1), with the circles representing the location of galaxy halos.

3. RESULTS

3.1. *Spatial Correlations*

Halo correlation functions ξ_{hh} along with some of the corresponding density correlations are plotted in Fig. 3. On scales larger than 1 Mpc, but comfortably smaller than the size of our models, the power law $\sim r^{-1.8}$ is a reasonable fit for all of the cases, except perhaps for the one with the largest quadrupole amplitude (cdm250b) which is most noticeably concave. It is also the only model which, at least on some scales, exceeds the observed amplitude of the galaxy-galaxy correlations. On smaller, sub-megaparsec scales, the halo correlation functions are noticeably less steep.

Halos are found to be less correlated than mass on megaparsec scales (Fig. 3b) in agreement with the results of Couchman & Carlberg (1992). This "anti-bias" is the result of the variation of the average halo mass with the density of the local environment: halos in denser regions are systematically more massive (see Fig. 4a), and are likely to be associated with more light (a similar effect has been noted by Brainerd & Villumsen (1992)). To take this into account, we have also shown one of the "halo-mass" correlation functions ξ_{hM} which is computed by weighting each of the halo contributions by their mass,

$$(1+\xi^i_{hM}(R)) \times 4\pi R^2 \delta R \;\sim \sum_{j\in[R,R+\delta R]} M_j. \tag{1}$$

That is, the contribution of the i'th halo is computed by summing over the total mass (rather than total number) of the halos which lie in the shell $R, R+\delta R$ (one could also define ξ_{MM} in an analogous manner). As is illustrated in Fig. 3c, ξ_{hM} is steeper than ξ_{hh}, which confirms our conclusions about the causes of the anti-bias exhibited by the halos. The dependence of the correlation function on the halo mass is also illustrated in Fig. 3c. As could be anticipated from our earlier arguments, more massive halos tend to be more clustered.

The volume density of halos as a function of their mass inside a 100 kpc radius from their center is plotted along with the Schechter function in Fig. 4b. When the halo mass is converted to luminosity by a mass to light ratio f of the stellar population and a dark to bright mass ratio D/B, then the resulting "luminosity" function is rather similar in shape and amplitude to the Schechter function usually employed to fit observations ($\Phi(L)dL = n_*(L/L_*)^\alpha e^{-L/L_*}dL/L_*$, $n_* \sim 1.2\times10^{-2}h^3Mpc^{-3}$, $\alpha \sim -1.25$, $L_* = 10^{10}L_\odot h^{-2}$). Thus we do not significantly overproduce sub–structureless, massive halos in our high resolution simulations in contrast to the findings of White et al. (1987) and Gelb et al. (1993). This conclusion is confirmed by the distribution of circular orbit velocities of our halos in our undernormalized $\sigma_8 < 1$ simulations: Out of $\sim 10^4$ halos per simulation only a few ($\sim 0.2\%$) have maximal v_{circ} above 550 km/s within 100 kpc, with the highest value being $\sim$ 700 km/s. We would like to stress that this encouraging agreement with the observations should not be overinterpreted. On the high mass end addition of baryonic "clumps" is likely to lower the merger efficiency. More importantly, on the low mass end the finite mass of the particles prevents us from doing justice to halos with masses less than $\approx 10^{11}M_\odot$.

3.2. *Peculiar Velocities from Simulations*

The rms pairwise peculiar radial velocities σ_v of the halos are shown in Fig. 5 as a function of the separation between them. When a normalization close to COBE is adopted ($\sigma_8 \simeq 1.1$) the relative velocity dispersions of halos at distances of the order of 1 Mpc are $\sim$ 800 km/s, a factor of $\sim$ 2 larger than the commonly accepted observational estimate of 340 km/s (Davis & Peebles, 1983). The one–dimensional halo velocity dispersions on megaparsec scales appear to be approximately proportional to σ_8 (see Table 1).

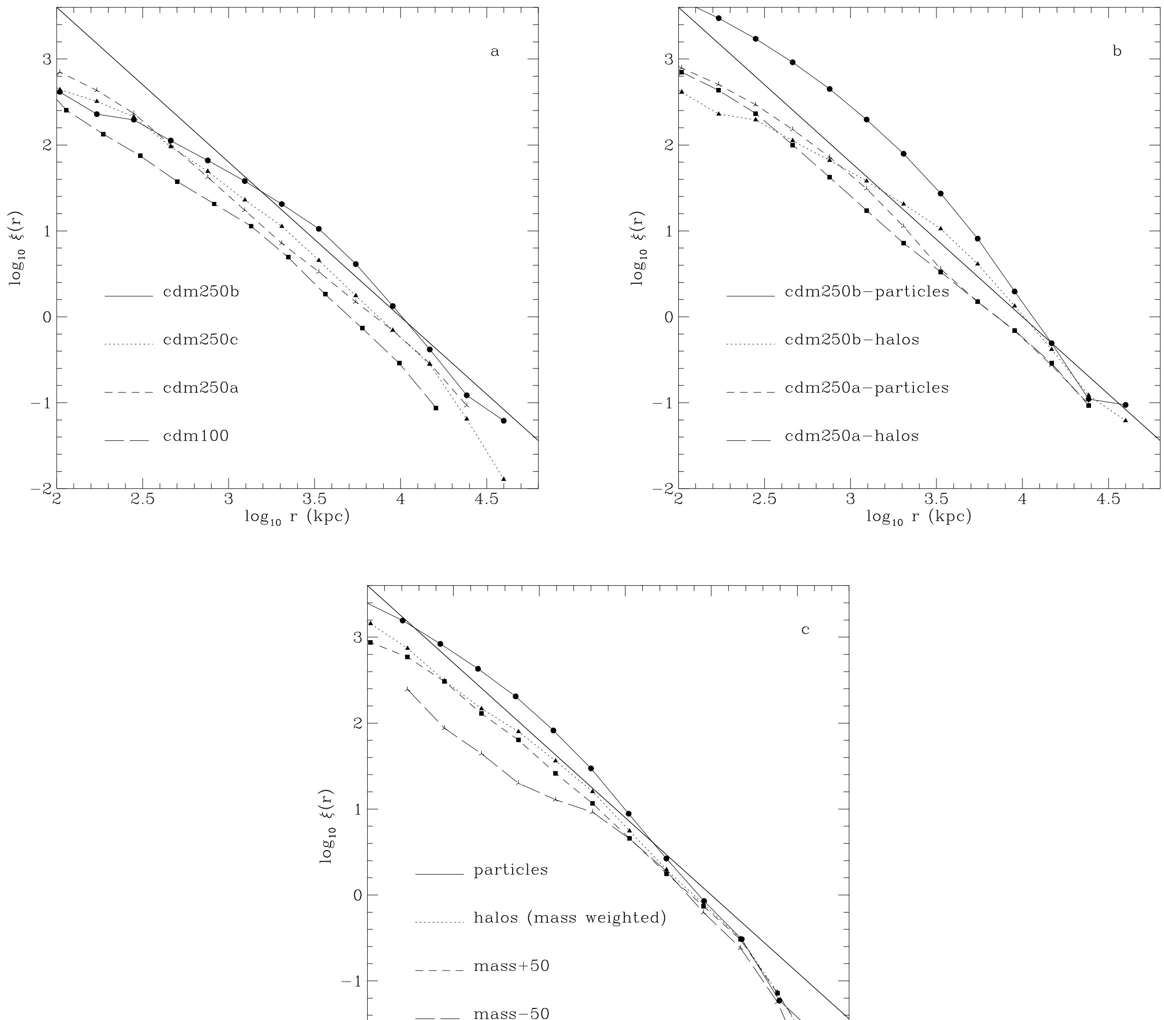

Figure 3: a) Halo correlations in the four models are plotted along with the usual fit ($\xi = (5\ h^{-1}Mpc/r)^{1.8}$) to the galaxy-galaxy correlation function. Note that the overnormalized model does not yield a power law. Shallower slopes on small scales are probably caused by mergers. Steeper slopes on the largest scales shown are most likely due to the finite size of our computational volume. b) Density correlations are compared with the halo correlations for the models with least and most power to illustrate anti-bias, which is caused by the systematic variation of the average halo mass with the average density of the neighborhood. (see Fig. 4). c) Halo correlations for two different mass bins and ξ_{hM} (see text) as well as particle correlations are shown for the run with the normalization closest to COBE.

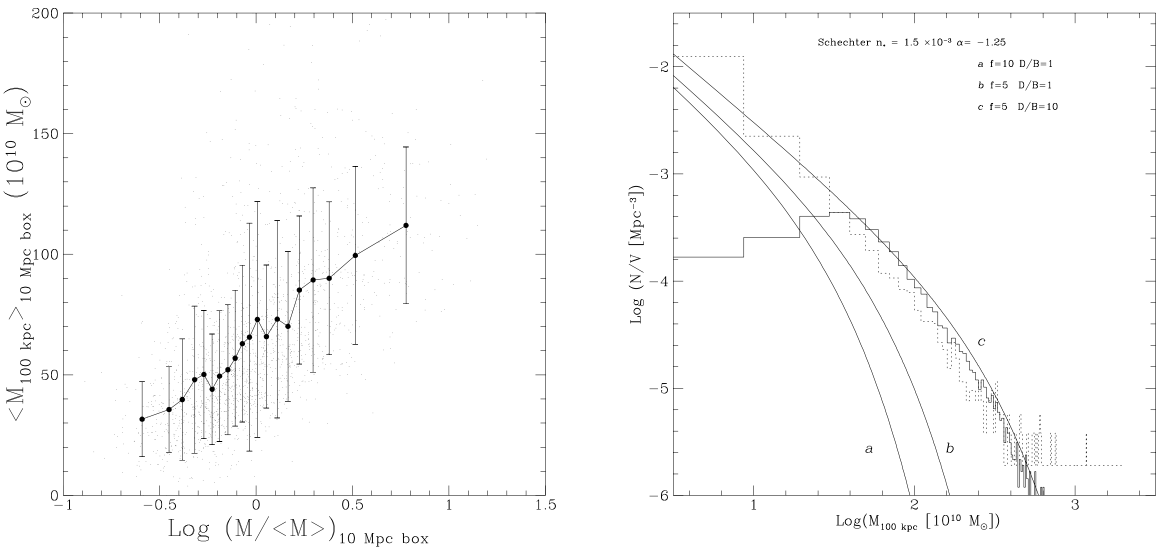

Figure 4: a.) The average mass of a halo in a 10 Mpc cube is plotted as a function of the total mass inside that cube. Averages over different "bins" with similar densities are connected with a heavy line with 1σ dispersion bars. This plot illustrates the systematic dependence of the mass of a typical halo on the average density of the environment — a bias which is responsible for the anti-bias of the correlation functions. b.) The mass distribution function (number per unit volume with mass between M and $M + \delta M$) for halos plotted along with Schechter functions for different assumed mass (in baryons) to light f and dark to bright D/B mass ratios. The agreement is quite good for $f = 5$ and $D/B = 10$. This corresponds to a net mass to light ratio $f \times D/B$ of 50. The solid histogram is for model cdm250a and the dotted histogram is for the highest resolution model cdm100.

We initiated our simulations motivated by the desire to eliminate what we have perceived as the only "weak link" in using σ_v as an argument against CDM — the identification of galactic halos with individual particles in nearly all previous numerical experiments. The discrepancy reported in the above paragraph appears to confirm the prevailing prejudice against COBE – normalized cold dark matter. Nevertheless, we have now — after careful analysis of our simulations and a re-analysis of the observations — come to the conclusion that σ_v is (i) a poor statistic, (ii) it is estimated from the observational data in a manner which differs from the way σ_v is computed from numerical experiments. Indeed, when the methods used to analyze the observations are applied to the halo catalogs obtained from the numerical experiments; (i) Estimates of σ_v vary significantly between distinct observation-sized halo samples, (ii) Values of $\sim$ 450 km/s are obtained for a significant number of samples extracted from the somewhat undernormalized ($\sigma_8 \simeq 0.7$) models at Mpc separations.

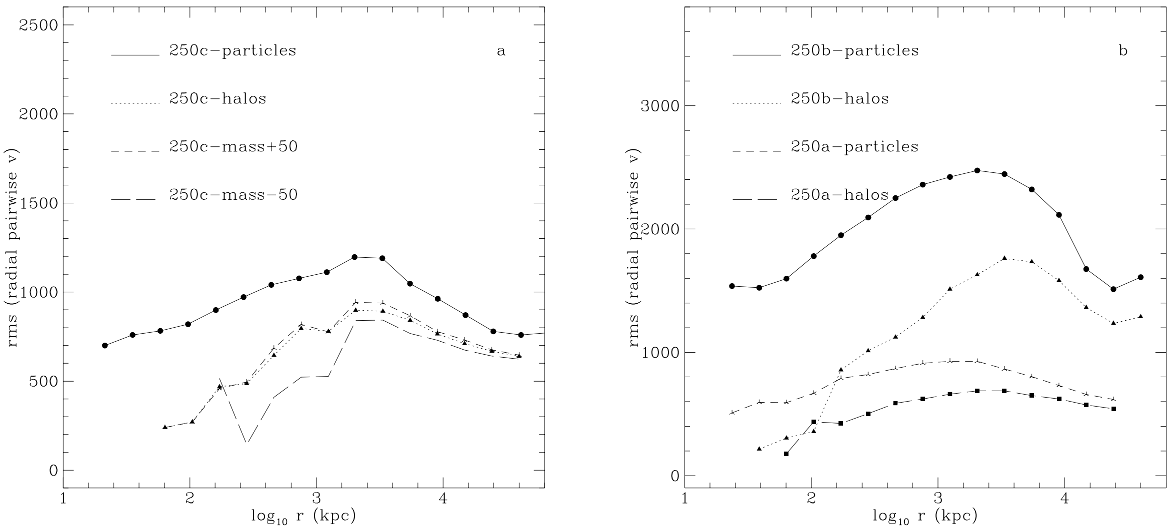

Figure 5: a.) One–dimensional relative peculiar velocities of halos and of particles in the model normalized closest to COBE. There is a significant, scale dependent velocity bias: the halos move less rapidly than the particles. Moreover, heavier (mass greater than $50 \times 10^{10} M_\odot$) halos move faster. b.) Particle and halo peculiar velocities for the models with largest and smallest normalization. Note the dependence of the velocities on distance for the two normalizations. The dispersion (σ_v) of the peculiar velocity about the mean for halos at 2 Mpc for all the models are tabulated in Table 1.

To some degree, the discrepancy between the observed and the usually quoted numerical estimates of σ_v are decreased by the velocity bias in our simulations. It is nearly a factor of two on 100 kpc scales, becoming somewhat smaller ($b_v \sim 0.7$) on megaparsec scales. This bias (first noted by Carlberg (1991)) is too large to be attributed solely to the differences between the motions of centers of mass of the collapsed objects and particles inside them. However, it is also too small to erase the difference between the usually quoted observational estimate of σ_v and the average halo motions obtained from our numerical experiments and shown in Fig. 5.

The reader should be cautioned that naive methods of estimating rms velocity dispersions (that is, averaging squares of the appropriate velocity differences and then taking the square root) are not correct, and would slightly (by 10-20% in our case) overestimate the σ_v derived from the observations. This is because the distribution of the pairwise radial peculiar velocities has both a substantial first and second moment. We illustrate this is Figure 6a, where the differences of pairwise radial peculiar

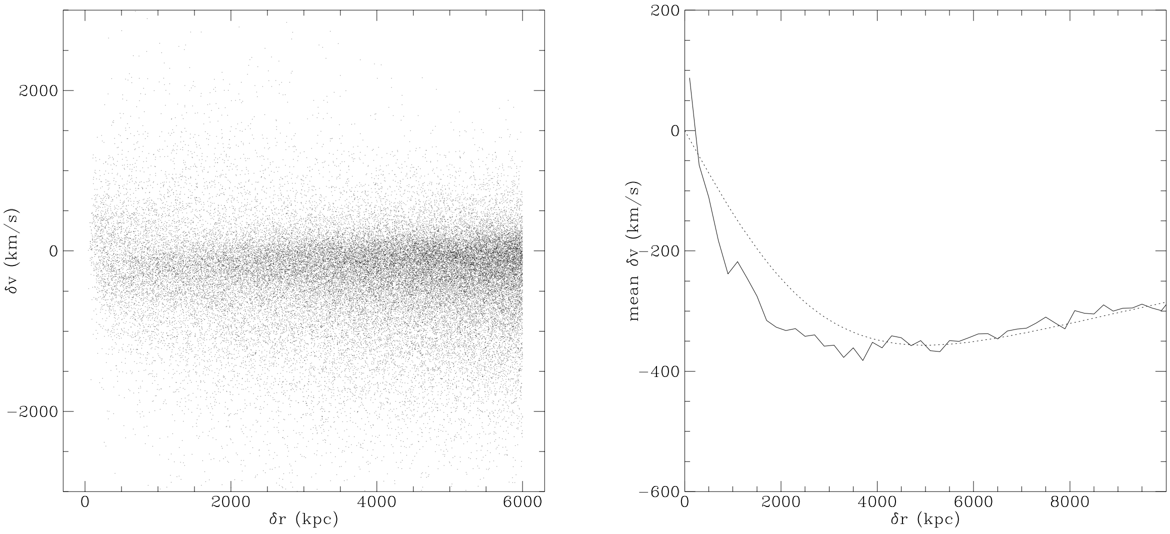

Figure 6: a.) The pairwise radial velocity differences for individual pairs are shown in this figure as a function of pair separation. Note that the velocity differences tend to be more often negative than positive, which results in the net infall. b.) Average value of the infall — the first moment of the distribution shown in Fig. 6a — is shown as a function of the separation between halos. On large scales the model used by Davis and Peebles (1983) seems to be a reasonable fit, but it does not yield accurate predictions on small (megaparsec) scales.

velocities are plotted as a function of distance for all of the pairs separated by less than 6 Mpc in one of the samples. When the average of these differences is taken, the separation dependent average infall shown in Fig. 6b is obtained.

The sought-after σ_v is the second moment of this distribution. It can be extracted from the data by computing a distribution of number of pairs as a function of their radial peculiar velocity differences. As is apparent in Fig. 7a, at Mpc separations this yields a distribution which is approximately exponential in Δv (hence the triangular shape on a logarithmic plot) and is symmetric about zero after the average infall (which results in a shift of the highest point of the triangle) is taken into account. Thus, the slope of the "folded" triangle shown in Fig. 7b can be used to obtain σ_v. We shall shortly see that this is in fact the basis of the method for extracting σ_v from the observations. Fortunately, for the naive method of estimating σ_v from the average of the differences of squares of peculiar velocities, at least in the models investigated here, the square of the first moment is quite small compared to the second moment of the velocity distribution. Consequently, the errors introduced by following the naive prescription for σ_v are quite small, and one does not need to worry about them too much.

The situation becomes considerably more complicated at larger distances (5 and 10 Mpc). There the "triangles" representing the logarithm of the distribution as a function of velocity differences are no longer isosceles. Hence, a simple formula for the distribution ($\exp(-|\Delta v|/\sqrt{2}\sigma_v)$) is no longer valid — at the very least, the two sides of the triangle have to be treated separately. This is an important conclusion for the observational estimates of σ_v as well, since the form of the radial pairwise peculiar velocity distribution function must be assumed in order to extract the value of σ_v.

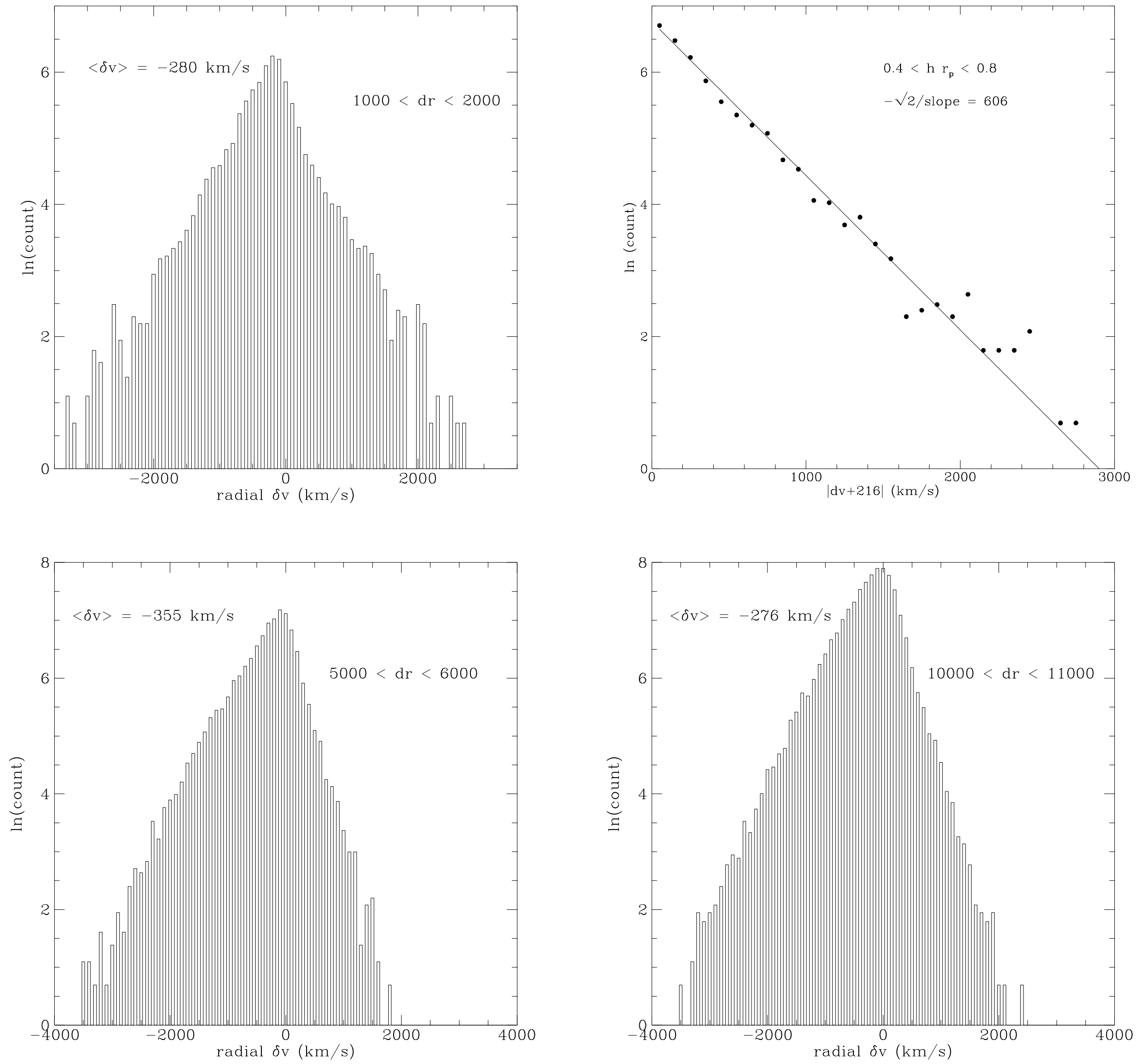

Figure 7: a). Distribution of the number of pairs as a function of pairwise radial velocity. The triangular shape of this histogram over a large range of δ_v implies that the distribution is indeed exponential, and the fact that the diagram appears isosceles allows us to infer σ_v from the slope of the "folded triangle" which is shown in b). There, the solid line (which is an excellent fit after the average infall of 216 km/s is subtracted) represents $\exp(-|\delta v|/\sqrt{2}\sigma_v)$ which yields $\sigma_v = 606$ km/s for this model. Figures c.) and d.) show histograms analogous to the one of Fig. 7a, but for larger separations. They are still triangular, but no longer isosceles, which will complicate any analysis of peculiar velocities on these scales. (see, e.g. Fisher et al. (1993)).

3.3. *Peculiar Velocities: Comparison With Observations*

The main reason for our conclusion concerning the viability of COBE-normalized CDM is that σ_v varies widely between different observation-sized samples of the *same* model, and that it is crucially influenced by the manner in which our models are analyzed, with numbers close to the observed ones resulting when the method outlined by Davis & Peebles (1983) is followed. In contrast to numerical experiments, which allow one to compute σ_v directly from the three-dimensional data on velocities and positions, observations provide one only with the angular separations and redshifts of galaxies. The method of Davis and Peebles is based on the comparison of the correlation functions in redshift with the correlation functions in the direction transverse to the line of sight. In the absence of peculiar motions, redshifts would translate directly to the line-of-sight distances and the two correlation functions would be identical. However, dispersion caused by peculiar velocities increases the spread in the redshift distribution. This increase in spread can be translated into a typical pairwise dispersion σ_v with the help of a few plausible assumptions, such as the form of the velocity distribution, see Fig. 7b.

In applying this procedure to the CfA survey Davis and Peebles have corrected the data for Virgocentric infall. This correction seems to be crucial, as it lowers the estimated σ_v from well above 500 km/s to below 400 km/s. The exact value of the estimated σ_v depends on one more correction, which accounts for the non-virgocentric, mean motion of galaxies towards each other caused by gravitational attraction, as well as on some other details of the analysis which do not seem to have too much impact on the estimates.

To arrive at the above conclusions concerning the viability of CDM we have cut out from our models samples with geometry and volume reminiscent of the CfA survey (Huchra et al., 1983) used to derive the most often quoted Davis–Peebles estimate $\sigma_v^{DP} = 340$ km/s at 1 h^{-1} Mpc (Davis & Peebles, 1983). Halos in these "samples" were then used to create catalogs of "galaxies", employing selection criteria analogous to those affecting observations (halo mass was assumed to be proportional to the luminosity of the "galaxy" inside it). Catalogs were created by selecting a CfA northern sky like "cone" with 1000 – 1400 sample halos from within the computational sphere. A selection procedure was implemented by identifying the luminosity of the halos with their mass, and then keeping all of the galaxies above a certain mass (absolute luminosity) inside 4000 km/s redshift, but only these galaxies with sufficient apparent luminosity beyond 4000 km/s. Velocities in the column labeled "DP" in Table 2 were computed using the method of Davis and Peebles, that is from the line of sight redshift and angular separations, but without eliminating (or correcting for) infall into clusters. Such corrections have proved crucial in obtaining low estimates of σ_v in our re-analysis of the CfA northern sky survey. The other column shows the estimate of the velocity dispersion of the same catalog of halos, but computed by using the known three-dimensional positions and velocities. As large portions of the volumes overlap, the above variations significantly underestimate the "cosmic" variations expected from truly independent samples in numerical experiments or — by the same token — in the real Universe. Pairwise velocity dispersions for galaxies separated by $0.8 < r < 1.6$ Mpc were then computed for each of our "catalogs" in several different ways. Pairwise velocity dispersions obtained with a full knowledge of three-dimensional positions vary between 600 and 800 km/s for 1 Mpc separations in the $\sigma_8 \simeq 0.7$ model samples. An even greater variation (from 450 to 850 km/s) occurs when the algorithm employed by Davis & Peebles (1983) is used to infer σ_v^{DP} (see Table 2). Moreover, both of these estimates are bound to depend critically on the treatment of the regions near rich clusters (which, in our simulations, have velocity dispersions near 1500 km/s). It is apparent that differences of σ_v between distinct "samples" of our model are much larger than the statistical estimates of the error inferred from any one of the samples.

For example, the formal standard deviation computed for σ_v^{DP} is 115 for the ten cdm250a slices and 197 for the eight cdm250c slices. The corresponding numbers for σ_v^{actual} are 79 and 81. It should be emphasized that both of these numbers underestimate the underlying standard deviation one would obtain from independent samples — our CfA-like slices overlap, so that approximately half of the (distant) volume is contained within each slice. Nevertheless, even these underestimated standard deviations are significantly larger than the formal statistical errors which are obtained from the least squares procedure, which presumably is the basis for the ± 40 km/s error estimate in the DP analysis.

cdm250a slice	DP	actual		cdm250c slice	DP	actual
1	577	610		1	662	1001
2	544	808		2	619	939
3	596	631		3	861	830
4	876	831		4	1082	907
5	464	670		5	757	970
6	453	703		6	1139	726
7	562	606		7	596	915
8	497	800		8	962	902
9	530	699				
10	643	673				

Table 2: Measured and actual velocity dispersions from CfA-like slices in the numerical models for $0.4 < hr_p < 0.8$.

Having verified its validity in such "artificial" catalogs, we have also applied our Davis–Peebles like algorithm to the observations. We shall report details of this analysis elsewhere. Let us note that when the sample is selected by directly interpreting redshift as a distance indicator for the computation of absolute magnitudes, σ_v for the CfA sample is 580 km/s. Selecting the sample in a more sophisticated manner which attempts to correct for Virgocentric infall when computing distance from redshift, results in $\sigma_v = 540$. In order to get a result close to the usually quoted 340 km/s we must either exclude galaxies within 10 degrees of the core of Virgo or subtract Virgocentric infall from the peculiar velocities. Needless to say, neither of these steps are used in the analysis of numerical experiments. It is perhaps useful to add that our conclusions concerning pairwise velocity dispersions in the CfA survey are consistent with the recent re-analysis of Mo et al. (1993).

It should be emphasized that without the Virgocentric infall correction, typical values of $\sigma_v \sim 500$ km/s or more inferred from the northern sky CfA survey are in reasonable accord with the similarly "uncorrected" estimates obtained from our numerical experiments. In view of these results it would therefore appear that there is no statistically significant discrepancy between the observations and predictions of the CDM/COBE model for peculiar velocities.

We feel that our cautionary remarks concerning the reliability of σ_v should be kept in mind when analyzing other data sets (such as the IRAS survey (Fisher et al., 1993)). We have not yet had a chance to apply these methods of analysis to that sample. However, in view of the above discussion, the use of IRAS galaxies is bound to under-represent cluster cores, which have had a decisive impact on the value of σ_v inferred from the CfA Northern Sky survey. Thus, we expect that the derived σ_v will underestimate the true "ensemble average" (to the extent to which such a concept even makes sense in view of our conclusions above). Moreover, extrapolation of the small-scale σ_v to $\sim 10h^{-1}$ Mpc scales (carried out in Fisher et al. (1993) and needing to extract average infall data) is likely to be affected by the asymmetry of the distribution of pairwise radial peculiar velocities we have detected on these scales (Fig. 7c-d).

4. DISCUSSION

Our simulations show anti-bias between halos and particles on small (megaparsec) scales. This result, while it appears to defy the popular wisdom, is, in retrospect, an easily understood consequence of merging, which is reflected in the systematic dependence of the halo mass on the larger-scale density of the environment. Anti-bias was previously reported in the dissipationless simulations of Carlberg (1991) as well as by Couchman & Carlberg (1992) who also attribute it to mergers. However, our halo correlation functions are rather different (more shallow) on small scales, which may be caused by the different numbers of particles per halo, and, consequently, different merging histories.

Correlation functions such as ξ_{hM} (Eq. 1) which weigh the contributions of halos with their mass (in numerical simulation) or — in the observational context — weigh contributions of galaxies with their inferred mass (i.e. from light or from the velocity dispersions) may turn out to be more closely related to the underlying mass distribution than the usual galaxy-galaxy correlation functions. Moreover, there is a noticeable dependence of the amplitude of the correlation function on the masses of the halos — heavier halos tend to be more correlated.

It should be emphasized that the anti-bias between the halos and the mass does not necessarily imply that there will be a similar anti-bias between galaxies and mass. This is because of the dissipative evolution of the baryonic component, which may result in gas clumps or in stellar systems compact enough to survive mergers of halos. Even if these clumps eventually merge, they could exist as separate entities much longer than individual halos, thus raising the amplitude of the correlation function on small scales. Hence, the bias seen by Cen & Ostriker (1992) and by Katz et al. (1992) must be largely a consequence of dissipative baryonic evolution. On the other hand, it is also possible that there are other, less physical reasons which could help explain at least some of the discrepancy. For example, the mesh code used by Cen & Ostriker (1992) loses resolution on sub-megaparsec scales, which is bound to suppress merging.

The relative velocities of halos on megaparsec scales are significantly smaller than the relative velocities of particles. This velocity bias decreases the discrepancy between the observational estimates of velocity dispersion and our numerical estimates for the cold dark matter model. The velocity bias we obtain is close to the one reported by Carlberg (1991) in a dissipationless simulation with a significantly lower resolution. More pronounced velocity bias $b_v = 0.37$ was obtained by Couchman & Carlberg (1992) for the "old" population of collapsed objects which had well-defined seeds at $z = 1$–3. On the other hand, our velocity bias is slightly more pronounced than the one reported by Cen & Ostriker (1992) who estimate $b_v \approx 0.8$ on megaparsec scales. This small discrepancy is not very significant statistically, and could be certainly attributed to the difference in the resolution between the two codes. Overall, there seems to be a significant consensus between these estimates of b_v obtained in several rather different simulations, using different numerical schemes and somewhat different physical input. Katz et al. (1992) report pairwise velocity dispersions of only 400 km/s on comparable scales for the COBE quadrupole normalization (which is somewhat less than $\sim$ 600 km/s we get for $\sigma_8 \simeq 0.7$), but detect no velocity bias. They attribute the smallness of their value of σ_v to the missing large scale power (their computational volume was only 22.222 h^{-1} Mpc on a side).

Perhaps the most important conclusion concerning σ_v is that the average pairwise peculiar velocity is an unreliable statistic. This is because, at least in our CDM models (but, most likely, also in our Universe (Mo et al., 1993)) σ_v differs significantly between regions usually sampled by the observations. Even more important is the manner in which the algorithm which is used to extract σ_v

from redshifts and positions deals with the clusters. The resulting correction has a major impact on the observational estimates, but, until now, was not applied to the analysis of numerical experiments. Thus, while the velocity bias we observe is insufficient to erase the discrepancy between the usually quoted $\sigma_v^{DP} \sim 340$ km/s and our estimates (which range between 600 and 800 km/s), the variation of estimates of σ_v between different samples — and especially, the dramatic impact of Virgocentric infall correction — makes it not only impossible to dismiss COBE–normalized CDM but appears to indicate a possible overlap (if not agreement) between the range of predictions of the model and observations. We intend to analyze this point in much more detail. Here, we only remark that, contrary to standard lore, the conflict between average σ_v in COBE-normalized models and the observational estimates of σ_v should not be regarded as a sufficient evidence to dismiss unbiased cold dark matter.

5. CONCLUSIONS

When the CDM spectrum is normalized to the anisotropies of the cosmic microwave background observed by COBE, collapsed objects forming in N-body simulations of $\sim$ 100 Mpc and $\sim$ 250 Mpc – sized fragments of a de Sitter Universe approximate the observed galaxy correlation function, but have somewhat smaller amplitudes, particularly on scales less than $\sim$ 1 Mpc. Their correlations are also smaller in amplitude than the density correlation function on megaparsec scales, but begin to coincide above $\sim$ 10 Mpc. Less massive halos tend to be more anti-biased in this manner. The one–dimensional radial pairwise velocity dispersion of halos σ_v has a dependence on distance qualitatively similar to observations and is approximately 200 km/s at 100 kpc, where it is nearly independent of normalization. On megaparsec scales it varies between $\sim$ 600 km/s for models normalized 1.5σ below the COBE implied value for mass fluctuations to nearly 800 km/s for fully normalized models. The velocity bias b_v is $\sim$ 0.5 at 100 kpc and approximately 0.7 at 1 Mpc.

The comparison between the numerical experiments and the observations is not as straightforward as it was usually assumed, both because of a significant scatter of σ_v between different observation-sized samples, and because of the importance of clusters. Moreover, when methods employed in the analysis of the observational data are implemented in the analysis of numerical experiments, estimates of pairwise velocity dispersions are often lowered, and exhibit large variations between different samples, eliminating the statistical basis for the usual claim of a conflict between the models and the observations.

We embarked on the study of CDM cosmology with a COBE prescribed normalization expecting to confirm the presently prevailing prejudice that without large bias the CDM model is untenable because it implies velocity dispersions on megaparsec scales which are too large to be reconciled with observations. This would have been our conclusion if halos were found to have relative velocities as large as those of individual particles, and of the same order as those predicted by the early "one particle — one galaxy" simulations (Davis et al., 1985). Instead we feel compelled, at the very least, to urge caution: CDM should not be dismissed prematurely, at least not on the basis of the small–scale velocity dispersions alone. Observations of relative peculiar velocities are still rather uncertain and difficult to interpret, and often yield values larger than the most often quoted estimate of 340 km/s (Davis & Peebles, 1983), which we were able to reproduce from the CfA Northern Sky survey, but only after removing the core of the Virgo cluster. Furthermore, observational data suggest (see, e.g. Mo et al. (1993), Hale-Sutton et al. (1989)) and our simulations confirm that σ_v may be a rather unreliable statistic. Thus, while our estimates of σ_v are similar to the one found in Cen & Ostriker (1992), our conclusion is much less negative for CDM. Indeed, it appears that CDM predicts pairwise relative velocities compatible with the observations, providing that both the simulations and the observations are analyzed in the same manner. This conclusion should be studied further, possibly using a better indicator of peculiar velocities than the average σ_v.

There are, of course, other observations which can be used to put constraints on cosmological models (see Table 3 for a brief and rather incomplete selection). For example, the abundance of Abell clusters has been used to argue for σ_8 of the order of (or even somewhat lower than) our undernormalized models (White et al., 1993; Weinberg & Cole, 1992). Similarly, low values of σ_8 (or, alternatively, a low Ω) seem to be favored by the recent estimates of the infall on $\sim$ 10 $h^{-1}Mpc$ scales (Fisher et al., 1993). By contrast, large scale streaming motions on similar scales (Dekel et al., 1990) appear to demand σ_8 close to the best COBE value. Before applying these results to rule out CDM, $\Omega = 1$ cosmology it is perhaps worth noting that no model can satisfy a set of constraints which are mutually inconsistent on more or less the same scale (as the bulk flows, Abell cluster abundances and infall velocities appear to be). Having said this, we would be inclined to favor a somewhat undernormalized, $\sigma_8 \approx 0.7$ flat CDM Universe as the best bet among the "standard" CDM models.

Scale (h^{-1} Mpc)	Test	σ_8
3000	$\Delta T/T$ (COBE)	0.9–1.3
20–50	Bulk Flows (POTENT)	0.8–1.2
10	Cluster Abundance	0.5–0.7
10	$\langle v_p - v' \rangle$	(0.3–0.5) [$\sim$ 0.7]
1	σ_v	(0.3–0.5) [$\sim$ 0.7]

Table 3: The preferred value of the normalizing constant σ_8 required to give the "right" amount of power in a CDM Universe on various scales according to several observational tests. These estimates were obtained on the basis of the unrealistic but simple assumptions that the initial power spectrum is purely Harrison-Zel'dovich, and that tensor modes (gravity waves) do not contribute to any of the tests. The last two rows give an "old" estimate of σ_8 based on low resolution simulations and a $\sigma_v^{DP} = 340$ km/s on 1 h^{-1}Mpc scale in parentheses and an estimate revised here in square brackets.

On a somewhat more speculative note it is worth pointing out that inflationary cosmology *does not* predict an *exactly* scale-invariant Harrison–Zel'dovich power spectrum. Only eternal inflation could yield $P(k) \sim k^n, n = 1$. The very fact that the Universe must leave the inflationary epoch implies $n < 1$. For example, chaotic inflation scenarios yield $n < 0.98$, with the two most popular variants — a quadratic and quartic potential for the inflaton field — yielding $n_2 = 0.97$ and $n_4 = 0.95$, respectively (Davis et al., 1992). This departure from the exact Harrison-Zel'dovich spectrum may seem inconsequential, but could be exactly what is needed to reconcile the COBE-measured $\Delta T/T$ with the CDM cosmogony: The "tilt" alone would lower the normalization of the initial power spectrum between the Hubble radius (where it is set) and smaller scales responsible for the formation of Abell clusters or 1 h^{-1} Mpc scales responsible for velocity dispersions. Moreover, the tilt $\delta n = 1 - n$ necessarily implies that a fraction $\frac{T}{S} = 7(1 - n)$ of the COBE DMR signal was due to gravitational wave (tensor) perturbations, which do not serve as seeds for structure formation (Davis et al., 1992). As a result of these two effects, instead of $\sigma_8 = 1.06$ (which seems to be the best estimate inferred from the COBE data, albeit with a 20% standard deviation) one has to lower $\delta M/M$ on the scale r by a factor $f \approx 1 + 7(1 - n) + (\frac{c/H}{r\ h^{-1}Mpc})^{1-n}$. Setting $r \sim 10\ h^{-1}$ Mpc, $n_2 = 0.97$ and $n_4 = 0.95$ yields $f_2 = 1.4$ and $f_4 = 1.68$, respectively. The resulting estimates of the "small scale σ_8" are then 0.76 and 0.63 — exactly what seems needed! Thus, the disagreement of the inflation-based CDM model and observations of small scale velocities seem to disappear when: (1) consequences of inflation are properly taken into account, and (2) observational data and numerical experiments are evaluated using the same procedures.

This research was primarily supported by a grant from NASA under the HPCC program. This research was performed in part using the Intel Touchstone Delta System operated by Caltech on behalf of the Concurrent Supercomputing Consortium. Access to this facility was provided by LANL and Caltech. JKS wishes to acknowledge support from the Advanced Computing Division of the NSF, as well as the CRPC. PJQ wishes to acknowledge support from the Australian DITAC bilateral science and technology program. Additional support from IGPP and the Aspen Center for Physics, where this paper was finished, is also acknowledged.

REFERENCES

Barnes, J., & Hut, P. 1986, Nature, 324, 446

Bertschinger, E., & Gelb, J. M. 1991, Computers in Physics, 5(2), 164

Brainerd, T. G., & Villumsen, J. V. 1992, Ap. J., 394, 409

Carlberg, R. G. 1991, Ap. J., 367, 385

Cen, R., & Ostriker, J. P. 1992, Ap. J., 399, L113

Couchman, H. M. P., & Carlberg, R. G. 1992, Ap. J., 389, 453

Davis, M., Efstathiou, G., Frenk, C. S., & White, S. D. M. 1985, Ap. J., 292, 371

Davis, M., & Peebles, P. J. E. 1983, Ap. J., 267, 465

Davis, R. L., Hodges, H. M., Smoot, G. F., Steinhart, P. J., & Turner, M. S. 1992, Phys. Rev. Let., 69, 1856

Dekel, A., Bertschinger, E., & Faber, S. M. 1990, Ap. J., 364, 370

Efstathiou, G., Bond, J. R., & White, S. D. M. 1992, M. N. R. A. S., 258, 1

Fisher, K. B., Davis, M., Strauss, M. A., Yahil, A., & Huchra, J. 1993, M. N. R. A. S. (submitted)

Gelb, J. M., Gradwohl, B., & Frieman, J. A. 1993, Ap. J. (Letters), 403, 5

Hale-Sutton, D., Fong, R., Metcalfe, N., & Shanks, T. 1989, M. N. R. A. S., 237, 569

Holtzman, J. A. 1989, Ap. J. Suppl., 71, 1

Huchra, J., Davis, M., Latham, D., & Tonry, J. 1983, Ap. J. Suppl., 52, 89

Katz, N., Hernquist, L., & Weinberg, D. H. 1992, Ap. J., 399, L109

Mo, H. J., Jing, Y. P., & Börner, G. 1993, M. N. R. A. S., 264, 825

Salmon, J. K., & Warren, M. S. 1994, J. Comp. Phys. (in press)

Smoot, G. F., Bennett, C. L., Kogut, A., & Wright, E. L. 1992, Ap. J. (Letters), 396, 1

Suginohara, T., Suto, Y., Bouchet, F. R., & Hernquist, L. 1991, Ap. J. Suppl., 75, 631

Villumsen, J. V. 1989, Ap. J. Suppl., 71, 407

Warren, M. S., Quinn, P. J., Salmon, J. K., & Zurek, W. H. 1992, Ap. J., 399, 405

Warren, M. S., & Salmon, J. K. 1992, in Supercomputing '92, Los Alamitos IEEE Comp. Soc.

Warren, M. S., & Salmon, J. K. 1993, in Supercomputing '93, Los Alamitos IEEE Comp. Soc.

Weinberg, D. H., & Cole, S. 1992, M. N. R. A. S., 259, 652

White, S. D. M., Davis, M., Efstathiou, G., & Frenk, C. S. 1987, Nature, 330, 451

White, S. D. M., Efstathiou, G., & Frenk, C. S. 1993, M. N. R. A. S., 262, 1023